

From A as in Aliasing to Z as in Zipper: Artifacts in MRI

Sabine Heiland¹

Abstract

A variety of artifacts may be encountered in MR images. They can be divided up into four major categories: (1) hardware-related artifacts, (2) sequence-related artifacts, (3) patient-related artifacts, and (4) artifacts of special MR techniques. This article discusses these types of artifacts, their derivations, their effects upon the MR image, and possible solutions to minimize them.

Key Words: Magnetic resonance imaging · Artifacts · Distortion · Motion artifacts · Fast imaging techniques

Clin Neuroradiol 2008;18:25–36

DOI: 10.1007/s00062-008-8003-y

Von A wie Aliasing bis Z wie Zipper: Artefakte in der Magnetresonanztomographie

Zusammenfassung

In MR-Bildern kann eine Vielzahl von Artefakten auftreten. Sie können vier großen Kategorien zugeordnet werden: 1. Hardware-bedingte Artefakte, 2. Sequenz-bedingte Artefakte, 3. von Patienten verursachte Artefakte und 4. Artefakte spezieller MR-Techniken. In diesem Artikel werden die oben genannten Haupttypen von Artefakten diskutiert. Dabei werden jeweils ihre Ursache und ihre Auswirkungen auf das MR-Bild erörtert und Wege aufgezeigt, wie man sie vermeiden oder zumindest minimieren kann.

Schlüsselwörter: Magnetresonanztomographie · Artefakte · Verzerrungen · Bewegungsartefakte · Schnelle Bildgebung

Introduction

Magnetic resonance imaging (MRI) is more susceptible to artifacts than other imaging techniques. This is in part due to the fact, that the MR signal depends on a variety of parameters: tissue parameters such as proton density, relaxation times, diffusion, presence of different molecules containing ¹H (e.g., water and fat), temperature; scanner parameters such as field strength, field homogeneity; sequence type and sequence parameters. This multiparametric dependency is the reason for the high and variable soft-tissue contrast. The drawback, how-

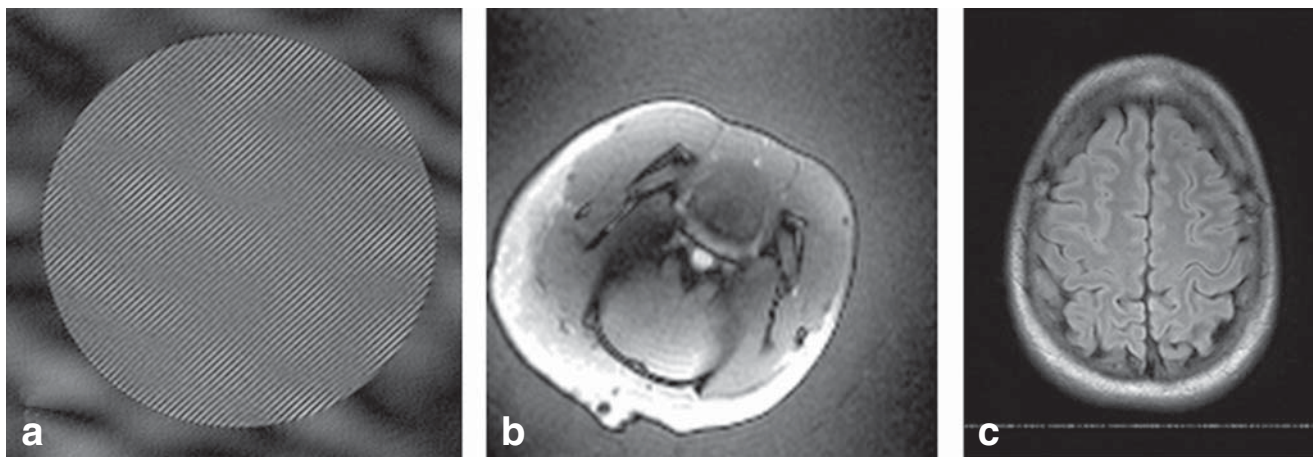
ever, is that unwanted effects may occur, if the MR sequence or hardware is not chosen properly.

MRI nowadays mainly uses the Fourier concept for spatial encoding: gradient fields are used for spatial encoding of the MR signal and an inverse Fourier transform (FT) for image reconstruction. This in turn results in a complex relationship between the artifact patterns and their origin. Therefore, it needs some knowledge about MR physics to fully understand the MR artifacts.

Good knowledge of MR artifacts is advantageous for three reasons: Firstly, for the operating personal,

¹Division of Experimental Radiology, Department of Neuroradiology, University of Heidelberg Medical Center, Germany.

Received: December 3, 2007; revision accepted: January 31, 2008



Figures 1a to 1c. Hardware-related artifacts: artifact patterns arising from a) spikes, b) data clipping, and c) RF leakage into the MR receiver (zipper artifact).

particularly for technicians, knowledge of MR artifacts may help to choose proper techniques that compensate for or avoid artifacts. Secondly, for physicians it is mandatory to know possible artifacts, because it allows them to distinguish between possible artifacts and pathologies affecting the MR signal. Finally, artifacts have often been the basis for development of new MR techniques: the knowledge of image disturbances can be used to specifically sensitize MR techniques to monitor morphology, function or metabolism.

Artifacts can be categorized in several ways. One way is to categorize them by the kind of signal contribution to the MR image (distortion, aliasing, signal loss, etc.). Another approach is to distinguish static from dynamic artifacts. In this article, the artifacts are classified by their cause or origin, as it allows to better understand how to avoid, to minimize or to compensate for artifacts.

Hardware-Related Artifacts

The common characteristic of hardware-related artifacts is, that there is no easy workaround by the user: as they are caused by technical defects of an MR component (gradient coil, amplifier, analog-digital converter, etc.), only a specialized service engineer can fix the problems.

Spikes

Spikes can occur in the raw data (k-space) of the MR image, if there is an electrostatic discharge somewhere in the receiver chain, e.g., between cables. As spikes result in one or several bright “spots” in the k-space, they form

regular, wave-like fringes within the MR image (Figure 1a). If the spike occurs close to the center of k-space, the fringes are broad, if the spike is close to the edge of the k-space, the fringes are fine.

If spikes occur, this may be due to defective components in the radiofrequency (RF) circuit. However, since dry air encourages the buildup of static electricity which in turn may discharge now and then during the measurement, dry air (below the humidity level specified by the manufacturer) within the scanner room may also be the cause of the spikes.

Data Clipping

If the receiver gain is set too high, the incoming signal at the analog-to-digital converter (ADC) is overloaded. This typically occurs at the central data points in k-space, since the maximum signal is measured there. As the center of the k space determines the total signal of the MR image, the FT generates some ghostly looking image with non-zero signal in the background (Figure 1b). This error may either occur, if the computer-controlled prescan process fails, or if the receiver gain is manually set to an improper value.

Zipper and Other Artifacts Due to External RF Sources

Artifacts can be caused by RF signals leaking into the receiver of the MR scanner. If the bandwidth of the interfering RF signal is low, such artifacts appear as a bright line in an MR image along the phase encoding axis (Figure 1c). Its position within the MR image depends on the frequency of the RF source that causes the artifact,

as well as on readout bandwidth and field of view (FOV). Broadband signals from external sources degrade the whole MR image. If the interfering signal has a further, low frequency component (e.g., flickering light bulbs in the scanner room), the result may be a spike within the MR image.

In general, interfering signals can arise from poorly shielded equipment inside the scanner room (anesthesia equipment, pulse oxymeter), or from RF sources outside the room, in case the Faraday shield has a leakage or a cabin door is not perfectly shut.

Sequence-Related Artifacts

Appropriate selection and use of MR sequences and sequence parameters is critically important for a good image quality. There are many potential sources of artifacts when choosing improper sequences or sequence parameters: some of these artifacts are easy to recognize, but some of them can mask pathologic conditions.

Aliasing

Aliasing (also known as *wraparound artifact*) occurs, if the FOV is smaller than the size of the imaged object. Volume elements outside the FOV experience a high field offset leading to a high frequency shift. If the sampling rate is lower than the expected maximum frequency range, this results in an inadequate sampling and reveals artificially low measured frequencies [1]. This in turn results in a spatial mismatching of the voxels outside the FOV to the opposite side of the image (Figure 2).

There are several ways to overcome this problem. The first is to increase the FOV to the size of the imaged object. Another way to avoid aliasing is to increase the sampling rate. In modern MR scanners this is automatically done in readout direction by using a sampling rate that is twice as high as the expected maximum frequency range. Furthermore, bandpass filters are applied which remove the higher frequencies. Therefore, there will be generally no aliasing in readout direction. In phase-encoding direction, the concept of oversampling is also applicable; using the double sampling rate, however, would result in double acquisition time. Therefore, in phase-encoding direction one mostly uses an oversam-

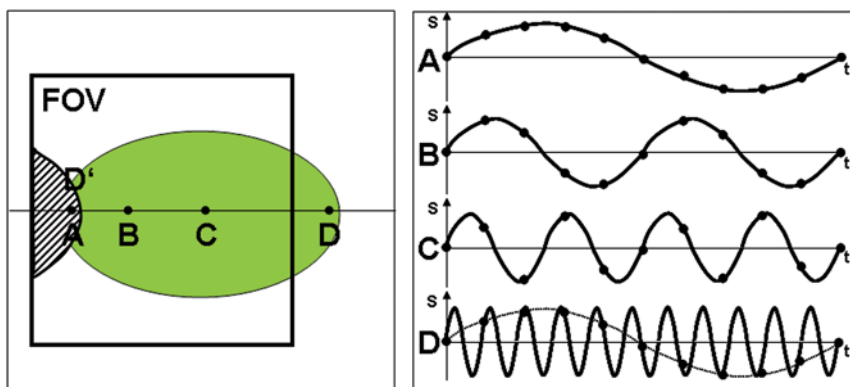


Figure 2. Aliasing artifact: by the gradient, the precession frequency is modulated along the line A–B–C–D. In points A, B and C, the sampling rate is high enough to register the data to a sinusoid with the correct frequency. In D, however, sampling ambiguity occurs, as the sampling frequency is too low compared to the actual precession frequency. The data are falsely allocated to a low frequency that equals the frequency at point A. Therefore, the signal of D is depicted in A.

pling factor of < 2 , which is adapted to the geometry and size of the object.

If the image object has different size in readout and phase direction, it often helps to swap readout and phase direction to match the phase direction with the shorter dimension of the object.

Another way to avoid aliasing is to use a coil with a spatially limited sensitivity profile (e.g., surface coils): if the sensitivity is close to zero outside the FOV, there will be no wraparound artifact even if the measured object exceeds the FOV. A similar approach is to use a presaturation pulse to saturate the spins outside the FOV.

In 3-D sequences, aliasing can also occur in slice direction, because spatial encoding in the slice direction is also done by phase encoding. In this case, the best way to avoid aliasing is to use a slab-sensitive excitation pulse (which only excites the 3-D slab) and a low oversampling rate of 10–20% to eliminate aliasing resulting from deviations of the real slice profile from the ideal boxcar profile.

Partial Volume Effects

This artifact occurs, if the voxel size is so large that it encompasses different tissue types. The signal intensity within such voxels equals the weighted average of both signal intensities; the weighting factor is the relative percentage of the tissue types within the voxel. In 2-D sequences, partial volume effects mainly occur in slice-encoding direction. In echoplanar imaging (EPI) sequences, different tissue types may not only result in intravoxel signal averaging, but also in intravoxel phase

dispersion, which in turn results in signal decrease.

Partial volume effects may decrease the visibility of small or low-contrast structures, reduce the accuracy of volumetry or simulate abnormalities.

Partial volume effects can be reduced by increasing the spatial resolution, particularly in slice direction. As this results in a reduction of signal-to-noise ratio (SNR), it is advantageous to use 3-D sequences instead of 2-D techniques, because they generally provide a higher SNR than 2-D techniques when applying the same sequence parameters (repetition time, spatial resolution). Therefore, acquisition of thin slices is possible without the need of several acquisitions; furthermore, no intervening slice gaps are needed. In EPI sequences, reduction in slice thickness may even result in an SNR increase because of less intravoxel dephasing.

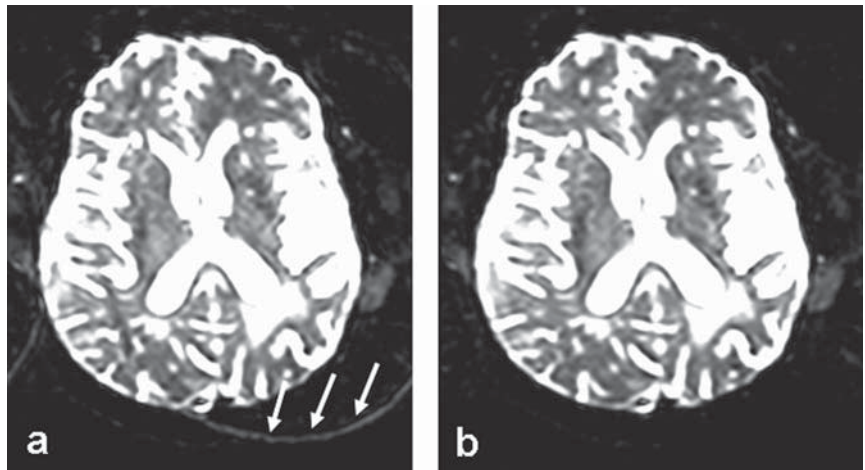
Crosstalk

Since the excitation pulse is relatively short (in the range of milliseconds or even less), the slice profile always deviates from the ideal boxcar profile and leads to partial excitation and saturation of the adjacent slices in 2-D sequences. This problem becomes particularly serious in multislice sequences with a short echo time (TE), because in this case the excitation or refocusing pulses in adjacent slices are applied with a very short time delay.

There are two ways to avoid this artifact; both can be used simultaneously. The first one is to use a gap between adjacent slice of 10–15% of the slice thickness. The second one is to excite the slices in an interleaved fashion, i.e., to first excite the slices with odd number and then the slices with even number. By this excitation scheme it is guaranteed that there is the maximum possible time gap between RF pulse application at two adjacent slices.

Saturation Artifacts

If the repetition time (TR) is much smaller than the longitudinal relaxation time (T1), severe saturation artifacts may occur, particularly if high pulse angles (α between 60° and 90°) are used for RF excitation. These artifacts limit the time resolution of dynamic MRI (perfusion



Figures 3a and 3b. Spin echo EPI scan of the brain with chemical shift artifacts in phase-encoding direction: a) the signal of the subcutaneous fat is displaced by several pixels (arrows); b) after fat saturation, this artifact has disappeared completely.

MRI, fluoroscopic MRI): therefore, dynamic imaging with a subsecond time resolution is generally performed using gradient echo sequences with low flip angles ($\alpha < 10^\circ$). Another application where saturation artifacts often appear is MRI with multiple oblique stacks, particularly within the spine. If these stacks overlap within the area of interest, saturation artifacts can mask the relevant information. Therefore, it is necessary to plan such multiple oblique stacks on an image perpendicular to the rotation axis of the stacks.

Chemical Shift Artifacts (1st Order)

Protons within different molecules “see” a slightly different magnetic field due to electromagnetic shielding by the molecule. Therefore, the Larmor frequency of water and fat differs; the relative frequency shift between the main fat peak and the water peak is 3.5 ppm.

This shift leads to a misregistration of fat and water pixels within the MR image, i.e., the signals of fat and water protons belonging to the same volume element are encoded as being located in different voxels [2].

The chemical shift increases with field strength, if all sequence parameters are kept constant. The number of in-plane pixels between fat and water protons of the same voxel is

$$\delta_{\text{pixel}} = \frac{\Delta\nu \cdot \text{MATRIX}_{\text{Read}}}{\text{BW}}$$

where $\Delta\nu$ is the chemical shift between fat and water protons, $\text{MATRIX}_{\text{Read}}$ is the matrix size in readout direction, and BW is the readout bandwidth of the sequence.

In standard sequences (with acquisition of only one phase-encoding line after each excitation), the chemical shift artifact occurs merely in readout direction. However, in EPI sequences bandwidth is lowest in phase-encoding directions. Therefore, in EPI sequences a huge chemical shift exists between water and fat protons (Figure 3a).

To reduce the chemical shift, one can increase the readout bandwidth. Since the bandwidth in phase-encoding direction is inherently low in EPI sequences, it is not possible to completely avoid chemical shift artifacts by increasing the bandwidth; therefore, in EPI sequences one gets around the chemical shift artifact by applying a fat suppression pulse (Figure 3b).

Chemical Shift Artifacts (2nd Order)

When using gradient echo sequences with certain echo times, there is a 180° phase shift between water and fat protons due to their different Larmor frequency. This *opposed-phase* condition occurs at

$$TE_{opposed} = \frac{2N - 1}{2 \cdot \Delta\nu \cdot \gamma \cdot B_0}, N = 1, 2, 3, \dots$$

where $\Delta\nu$ is the relative frequency shift between water and fat protons ($\Delta\nu = 3.5$ ppm).

At this echo time, the signal of water and fat cancels out in voxels with equal signal contribution of fat and water protons leading to a “black boundary” around fatty tissues. This effect is called 2nd order chemical shift artifact [3].

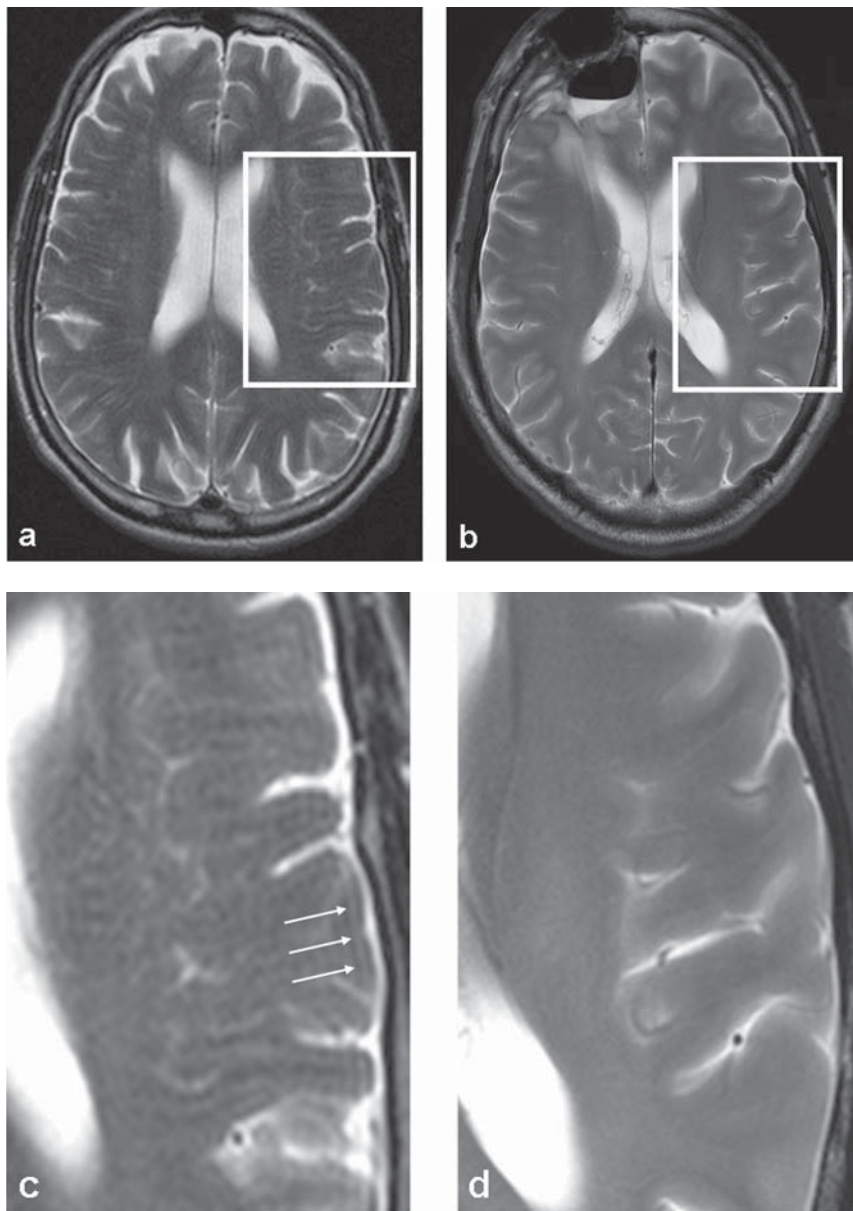
This artifact can be avoided by using echo times that fulfill the in phase condition

$$TE_{opposed} = \frac{N}{\Delta\nu \cdot \gamma \cdot B_0}, N = 1, 2, 3, \dots$$

Truncation Artifacts (Gibbs Ringing)

This artifact occurs, if there are structures where the signal intensity

changes considerably and abruptly. Such sharp edges result in high amplitudes at high spatial frequency, i.e., at the outer parts of the k-space. If sharp signal intensity discontinuities are sampled with a low spatial frequency (i.e., low spatial resolution), the reconstructed image differs from the original object, because the high-frequency components are missing. This results in a periodic over- and undershoot of signal intensity



Figures 4a to 4d. Influence of spatial resolution upon Gibbs ringing artifact: a) T2-weighted TSE image with a matrix size of 256 × 256; b) T2-weighted TSE image with the same FOV as in a, but a matrix size of 512 × 512; c) detail of a, showing distinct Gibbs ringing artifacts (arrows) arising from the sharp signal changes between skull, cerebrospinal fluid and brain matter; d) detail of b, showing no Gibbs ringing artifacts.

around the structure which causes the artifact (Figures 4a and 4c) [4].

This artifact cannot be avoided completely, as the sampled MR data are always assigned to a k-space matrix with a finite number of elements. By increasing the spatial resolution, however, the frequencies of the signal over- and undershoot become much lower and less prominent (Figures 4b and 4d). Nowadays, enhanced MR scanner hard- and software such as high magnetic field, high and fast gradients and parallel imaging techniques allow to acquire MR images with high spatial resolution in reasonable acquisition time. Therefore, truncation artifacts occur less often than in the early days of MRI and can merely be found in functional and dynamic imaging, where spatial resolution is inherently low, as acquisition time has to be very short.

Patient-Related Artifacts

Motion Artifacts

Motion is the most prevalent source of imaging artifacts. When spins are moving, the total integral over the magnetic field experienced between excitation pulse and echo collection differs from that of spins at rest (phase errors, cf. Figure 5a). This causes incorrect allocation of the signal within the k-space and in turn artifacts within the reconstructed MR image.

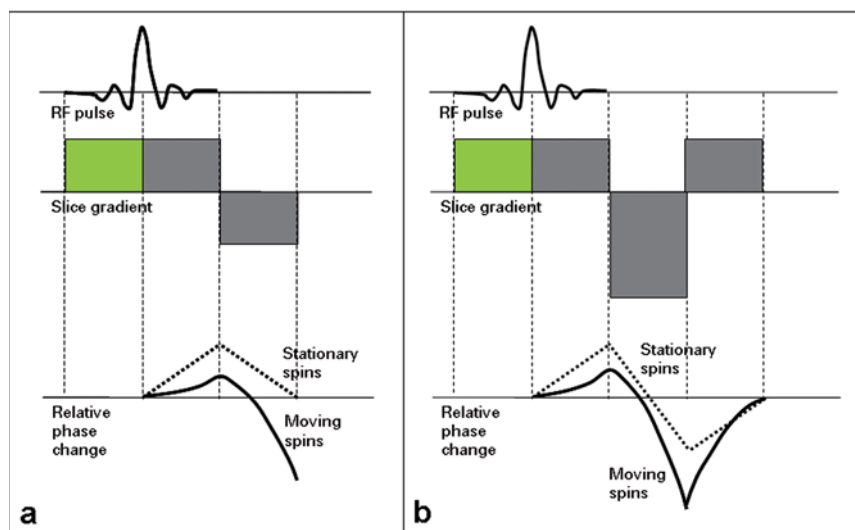
There are basically two types of patient motion: one is irregular bulk motion of the body or parts of the

body (e.g., peristalsis of the gastrointestinal tract), the second type is regular motion with continuous velocity or periodic velocity changes, particularly the steady or pulsatile blood flow. The artifact patterns resulting from irregular motion are unpredictable. Body motion results in a blurred image with ghosts in phase-encoding direction. Pulsatile motion, on the other hand, results in a predictable signal pattern: it produces replicas of the pulsating structure at abnormal positions. If the pulsation is sinusoidal (i.e., the velocity can be described with a sine or cosine function), the distance between pulsating object and ghost is proportional to the pulsation rate [1]. Complex motion, e.g., the aortic blood flow, can be decomposed in several sinusoids of different pulse rate and amplitude; such motions produce multiple ghosts, and distance to object and signal amplitude depend on the pulse rates and relative amplitudes of the particular components.

As motion artifacts may arise from different origins, there are several ways to avoid or compensate for them.

One way to avoid motion artifacts is to reduce the cause of the artifact to a minimum, at least for the duration of the image acquisition. Involuntary bulk motion of the gastrointestinal tract can be prevented by application of antispasmodic drugs. Artifacts by respiratory motion can be reduced by using short sequences during breathhold. Furthermore, these artifacts can be minimized by signal averaging in the same way that multiple averages increase the SNR [1].

Motion artifacts by blood flow can be easily reduced by presaturation of the blood inferior and superior to the measured slice package, respectively. By presaturation, flowing blood has less longitudinal magnetization and hence contributes less to the resulting MR signal than stationary tissue. As blood flow is a regular motion of spins, one can determine the phase error of constant or pulsatile flow. In turn, one can modify the gradient scheme in order to prevent phase shifts of motion with constant velocity, constant acceleration, etc. (cf. Figure 5b). This involves application of complex waveforms of the dephasing and rephasing gradient to



Figures 5a and 5b. Motion artifacts, exemplarily illustrated for the slice gradient: a) in the standard sequence, stationary spins are rephased once the slice gradient is completed, whereas there is a residual dephasing in spins moving, e.g., with constant velocity; b) with the more complex gradient scheme of the gradient moment nulling, both stationary and moving spins are completely rephased.

correct for higher orders of motion [5]. The theoretical basis for this *gradient moment nulling* technique is that the phase error $\Delta\Phi$ arising from the motion within a gradient field $G(t)$ can be written as a Taylor series:

$$\Delta\Phi = k \cdot \int x(t) \cdot G(t) dt = k \cdot x_0 \underbrace{\int G(t) dt}_{0 \text{ (at echo)}} + k \cdot \left. \frac{\partial x}{\partial t} \right|_{x=x_0} \underbrace{\int t G(t) dt}_{1^{\text{st}} \text{ order moment}} + \frac{k}{2} \left. \frac{\partial^2 x}{\partial t^2} \right|_{x=x_0} \underbrace{\int t^2 G(t) dt}_{2^{\text{nd}} \text{ order moment}} + \dots$$

At the time of the gradient echo, the first integral equals zero. With a proper design of the gradient waveform the 1st order moment (= second integral) becomes zero (Figure 5b). In this case spin motion with constant velocity does not produce any artifact. For 2nd order gradient moment nulling the requirements to the gradient profile become even higher, because also the 2nd order moment has to be zero.

The disadvantage of such gradient moment nulling techniques is the prolongation of the minimum TE, because additional time is needed to fit in the extra gradient lobes. Furthermore, the maximum gradient and the maximum slew rate used in certain sequences may be increased by gradient moment nulling. This in turn limits the FOV or the slice thickness for a given TR.

One easy and efficient way to prevent motion artifacts of certain structures from masking the tissue or organ of interest is to swap the readout and phase-encoding direction: changing the phase-encoding direction to left-right in axial slices for instance helps to minimize the effect of eye movement, as the ghosts caused by motion do not interfere with the brain signal.

If the motion is periodic and the source of motion can be recorded, triggering is a good alternative to the workarounds mentioned above. At present, there exist robust methods for respiratory, pulse and ECG gating. Since the data are not sampled continuously but only in time intervals with no or little motion, the acquisition time of gated sequences is significantly longer and repetition time may be no longer constant.

When applying motion-sensitive MR techniques such as diffusion-weighted MR imaging, it is advantageous to use MR sequences that are less prone to motion artifacts than conventional sampling techniques. One way of doing so is to use ultrafast sequences like EPI. In addition to that, one can apply *navigator echoes*: with this method, one acquires an additional line of data which is not phase-encoded and gives information about the spatial location of the spins [6].

This allows to retrospectively correct for the phase error due to motion. A third class of techniques that are less sensitive to motion are projection-reconstruction imaging techniques such as PROPELLER (*periodically rotated overlapping parallel lines with enhanced reconstruction*). With this method, the central region of the k-space is sampled several times during image acquisition. This leads to a motion artifact suppression by averaging. Furthermore, the central point information can be used to perform retrospective phase error corrections [7].

Susceptibility Artifacts

These artifacts occur, if the static magnetic field is not perfectly uniform. Such nonuniformities may be a result of imperfections in the magnet itself; more often, they are due to the imaged object: at boundaries between tissues with different magnetic susceptibilities (e.g., air/soft tissue), the magnetic field is distorted, i.e., there are macroscopic field gradients. Since the susceptibility of metal is much higher than that of soft tissue, even stronger artifacts are seen around metallic, particularly ferromagnetic objects within the body [8].

As a result of these macroscopic field gradients, dephasing of spins within the voxel becomes faster, which in turn leads to gross signal decrease up to complete signal loss. Furthermore, the shift in the effective magnetic field leads to misregistration of the signal within the raw data, which in turn leads to distortions. It is important to keep in mind that these distortions might also occur perpendicular to the acquired slice, which mostly is less obvious than in plane distortions and may lead to false diagnoses.

Susceptibility artifacts increase with echo time and field strength and are most prominent in gradient echo and in echoplanar imaging (Figure 6).

To reduce susceptibility artifacts, one should basically use spin echo instead of gradient echo sequences. Also reduction of echo time and increase of the readout bandwidth helps to keep susceptibility artifacts as small as possible. In applications based on susceptibility contrast (e.g., functional MRI), other techniques have to be used for reduction of susceptibility artifacts: Z-shimming and optimization of the imaging slice orientation are particular methods to reduce artifacts without affecting sensitivity [9].

Changes in field strength due to susceptibility differences may also lead to imperfect fat saturation, if the shift in resonance frequency is larger than the band-

width of the fat saturation pulse [10]. This may occur in patients with metallic implants or braces, but also in regions where the patient diameter changes significantly (e.g., in the region between head, neck and shoulder). In this case, one can perform a slice-specific shimming procedure. If this does not help, fat saturation should either be performed by inversion recovery methods (short TI inversion recovery [STIR]) or by using opposed-phase gradient echo techniques [3, 10].

Artifacts of Special Sequences

Besides artifacts that may occur independent of the sequence used, there are certain sequence types that are

more prone to artifacts than others. In particular fast imaging sequences and motion-sensitized sequences (MR angiography [MRA], diffusion MRI) are highly susceptible to phase errors which result from field inhomogeneity or patient motion.

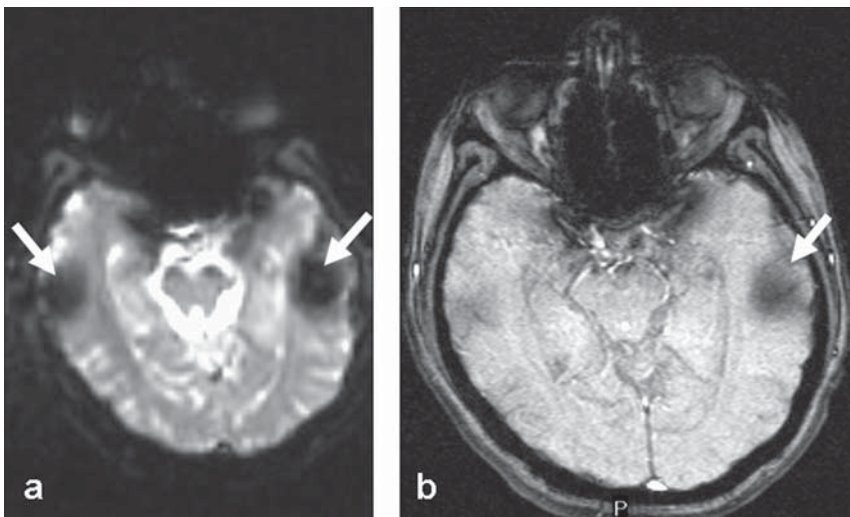
Blurring in TSE Sequences

Turbo-spin echo (TSE) sequences reduce acquisition time significantly by collecting multiple echoes per RF excitation. Therefore, the scan time is cut down by a factor that equals the echo train length (ETL). On the other hand, the echo time of the image is no longer defined precisely. Instead, the effective echo time (TE_{eff}), which equals the echo time of the k-space center, is characterizing the weighting of the respective sequence.

If ETL is high, blurring and contrast loss will occur. This results from the fact, that there are large differences in the actual echo time from the first to the last line of k-space. These differences are the higher, the lower the readout bandwidth and the higher the echo train length. Furthermore, the overall echo time difference in k-space is the higher, the lower the effective echo time, because at low echo times there is still a huge signal decay, whereas at high echo times signal does only change slightly with echo time (cf. Figure 7). Therefore, ETL in T1-weighted TSE sequences should not exceed 5–7, whereas T2 sequences can be performed with an ETL up to about 15 without any significant blurring artifacts.

Stimulated Echo Artifacts

Trains of periodic RF pulses may produce stimulated echoes, which interfere with the spin echoes and produce a pattern of fine lines. Such artifacts occur mainly in TSE sequences, because many RF pulses are applied within a short time. Particularly if the readout bandwidth is small, stimulated echoes may be



Figures 6a and 6b. Susceptibility artifacts (arrows) resulting from field inhomogeneities arising from the outer ear hole: a) gradient echo EPI and b) T2*-weighted gradient echo sequence.

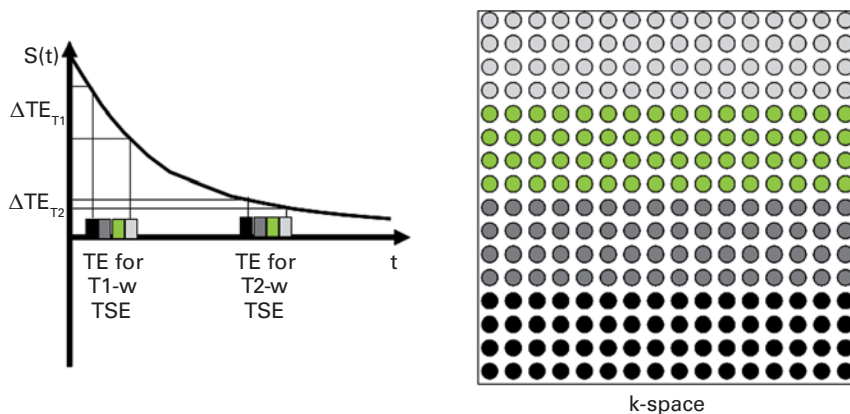


Figure 7. Signal change between the domains of k-space acquired at different echo times. At short echo times, that are used for T1-weighted TSE, signal change is large, whereas it is small for large TE used for T2-weighted TSE. Therefore, T2-weighted TSEs are less blurred than T1-weighted TSEs, if the same ETL and readout bandwidth are used.

captured within the readout time interval. Increasing the bandwidth or changing the echo time of the first echo helps to push the unwanted stimulated echoes outside the readout window. Another way to avoid stimulated echo artifacts is spoiling of transverse magnetization after each echo acquisition by gradients or RF spoilers [11].

Another source of stimulated echo artifacts may be crosstalk of adjacent slices: protons at the borderline may be exposed to the RF pulses of both slices; this pulse train again may produce stimulated echoes. For this purpose an increase of the interslice gap or interleaved slice excitation helps to avoid the artifact.

Saturation Artifacts in MRA

Time of flight (TOF) MRA is based on the fact, that pulses with short repetition time saturate the stationary tissue, which in turn results in signal loss, whereas protons in fresh, unsaturated blood can flow into the slice hence resulting in hyperintensity of the vessels. However, if slice orientation or sequence parameters are not chosen properly, saturation effects within the vessels of interest may occur. If the pathway of the vessel through the slice has the length L_{vessel} , the RF-saturated blood within that vessel will not leave the slice completely if

$$L_{\text{vessel}} > v_{\text{blood}} \cdot TR ,$$

where v_{blood} is the velocity of the blood flow within the respective vessel. In such case the contrast between vessel and surrounding tissue will diminish.

As in 2-D TOF sequences the slice thickness is in the range of millimeters, saturation artifacts rarely occur, given that the slice excitation order is chosen opposed to the direction of blood flow. In 3-D TOF sequences, however, the excited slab (= stack of slices) is much larger, i.e., in the range of centimeters; therefore, saturation effects occur even in vessels with high blood flow (Figure 8). A possible way to avoid saturation is to use the MOTSA technique (multiple overlapping thin slab angiography) [12], which divides up the large 3-D slab into several, partially overlapping 3-D slabs. Saturation of spins during the passage through the slab can also be diminished by ramped flip angles: the flip angle of the RF pulse is linearly increased from the proximal to the distal end of the 3-D slab to guarantee the same tissue-vessel contrast along the vessel [13]. Finally, by using contrast agent, one can selectively reduce T1 within the vessels and thus reduce saturation artifacts.

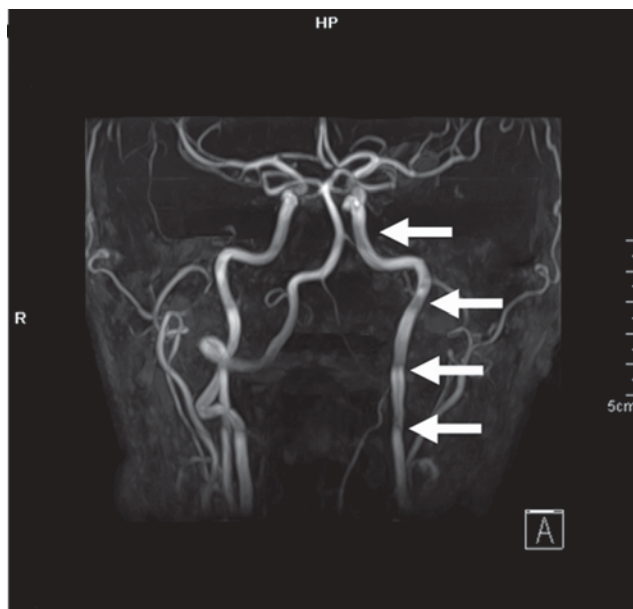


Figure 8. Saturation artifacts in 3-D MR TOF acquisition using the MOTSA technique: the slab thickness of the overlapping 3-D slabs has been chosen too large; therefore, the spins in blood partly saturate resulting in a periodic pattern of signal loss within the vessels.

Dephasing Artifacts in MRA

At certain points in vasculature, e.g., at stenoses, vessel branches and within aneurysms, flow is no longer laminar but becomes turbulent. In such turbulent regions, different protons within the same voxel have passed through different gradient field. This results in phase dispersion of the transverse magnetization, which in turn leads to signal loss. Intravoxel dephasing can also occur at the boundaries of the vessel lumen, because the radial velocity gradient is largest close to the vessel wall. Intravoxel dephasing artifacts are the reason for overestimation of stenoses and underestimation of the vessel radius [14].

Dephasing artifacts can be reduced by using a shorter echo time. Furthermore, reducing the voxel size helps to keep the phase dispersion at a lower level. Finally, contrast-enhanced MRA is much less prone to intravoxel dispersion artifacts than TOF and phase contrast techniques, because the dominating effect is the T1 effect, which is not influenced by turbulent flow or gradients in flow velocity.

EPI Ghosting

Data readout in EPI requires fast switching of high field gradients. These field variations produce eddy currents.

As the gradient polarities for the odd phase-encoding lines and the even phase-encoding lines differ, there are a resulting misalignment and phase variations between odd and even echoes in k-space. Within the reconstructed MR image, this k-space shift is reflected in a ghost shifted by FOV/2 pixels from the original structure (Figure 9).

EPI ghosting can be reduced by careful adjustment of the gradient waveform and timing (preemphasis) [15]. Also the acquisition of a reference scan can help to minimize EPI ghosting [16]; the phase information obtained from this reference scan is used while post-processing the EPI data. Nowadays, in whole-body MR

scanners the correction methods are performed in an automatic fashion.

EPI Distortions

EPI sequences have a rather low bandwidth (i.e., a long readout time span) in phase-encoding direction. Therefore, even small magnetic field inhomogeneities produce large phase shifts. These phase shifts result in distortion of the measured object within the EPI scan (cf. Figure 10).

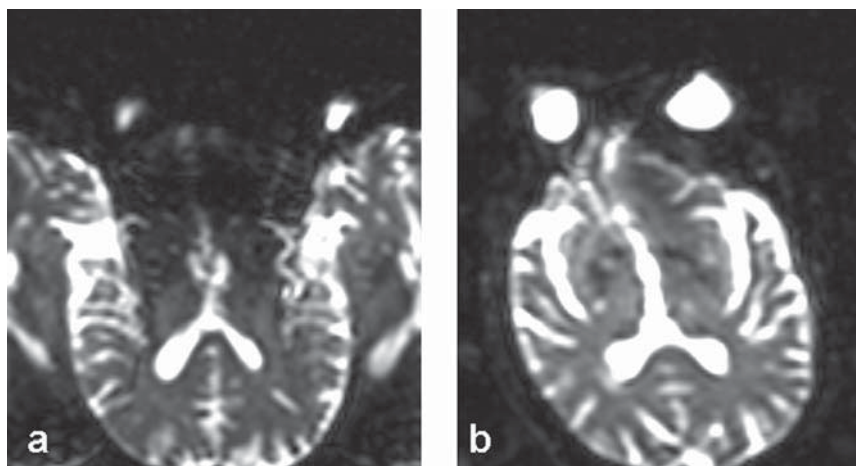
As the distortions are nonlinear, they cannot be compensated for by image registration methods. However, there are several ways to minimize distortions. (1)

The magnetic field within the volume of interest should be homogenized prior to the EPI scan. This can be done by volume shim methods. (2) With multiecho gradient echo sequences one can calculate maps of the magnetic field. With this information, it is possible to correct the EPI scan for the effects of static field inhomogeneities [17]. (3) Multichannel modulation as proposed by Chen & Wyrwicz [18] allows to correct for the distortions directly in k-space. Contrary to the field map method, multichannel modulation also corrects for dynamic effects, e.g., eddy current artifacts. However, this method needs long acquisition time, because $2N_y - 1$ correction datasets are necessary, where N_y is the number of phase-encoding steps within the EPI scan.

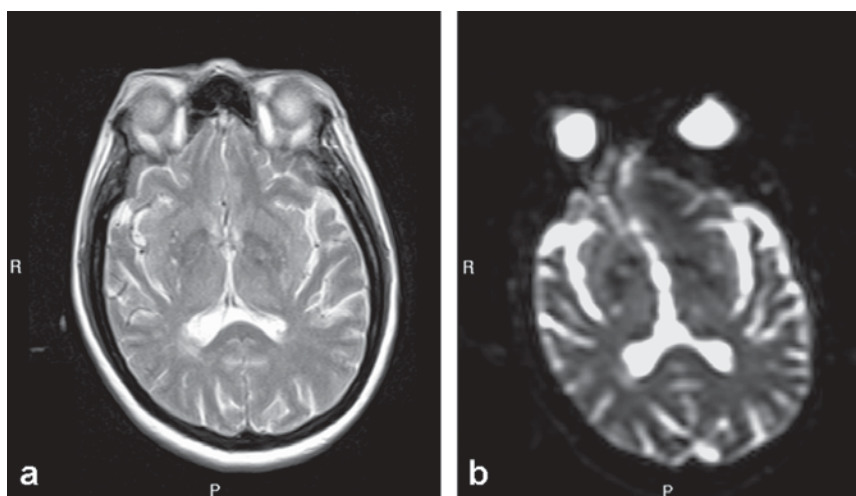
Dielectric Effects

When using MR systems with high field strength ($B_0 \geq 3$ T), the high resonance frequency implies that the RF wavelength becomes comparable to the object size. The high dielectric constant of tissue further reduces the RF wavelength within the object and results in generating standing waves, which in turn leads to spatial variations of the B_1 field [19].

This inhomogeneous B_1 field distribution results in nonuniform



Figures 9a and 9b. EPI ghosts a) before and b) after correction. The ghosts are shifted by FOV/2 from the original location.



Figures 10a and 10b. Axial MR images of the brain acquired with a) a T2-weighted TSE sequence and b) a spin echo EPI sequence. The frontal part of the brain and the eyes are distorted in the EPI scan caused by magnetic field inhomogeneities in the region of the frontal sinus.

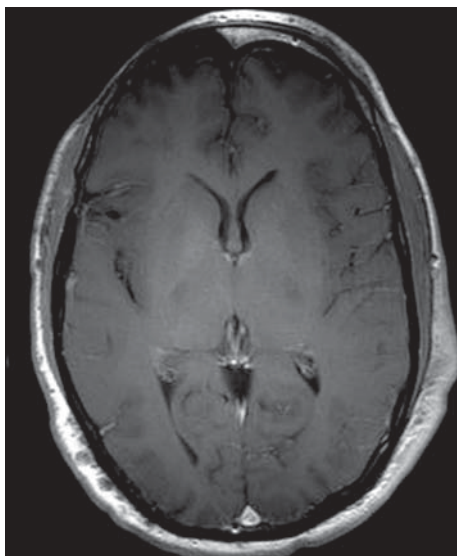


Figure 11. Axial T1-weighted MR image acquired at a 3-T MR scanner. The signal profile within the brain is inhomogeneous due to dielectric effects occurring at high field strength.

flip angles over the imaged slice, which in turn results in inhomogeneous signal profiles (Figure 11).

The most promising way to avoid this problem is to use multichannel transmit and receive coils [20]. The development and optimization of such multichannel coils is of highest importance for the application of whole-body MR scanners with a field strength of ≥ 7 T. Alternatively, one can use sequences which are less sensitive to B_1 field inhomogeneities [21] or use special pulse shapes producing a more homogeneous B_1 field [22].

Effects or Artifacts?

Artifacts have not only been a driving force for the development of new MRI techniques that avoid or minimize those artifacts, but have also been a source for new imaging techniques that use the particular sensitivity earlier seen as an “unwanted” artifact as a “wanted” effect for certain applications.

One example are susceptibility artifacts: such artifacts may disturb the MR image, but on the other hand, they are the basis for BOLD (blood oxygenation level-dependent) imaging as well as for bolus-tracking methods to measure brain perfusion [23]. Furthermore, SWI (susceptibility-weighted imaging), which can be used both for venography and for detection of blood within the brain, is based on the high sensitivity of MRI to magnetic field inhomogeneities [24]. Another example

are motion artifacts: although one tries to minimize the inherent motion sensitivity of MRI in standard MR sequences, certain techniques such as phase contrast imaging and diffusion-weighted imaging are particularly sensitized to small motion to display blood flow or the Brownian motion of water [25].

Conclusion

Artifacts occur frequently in MRI. Although in most cases they only degrade image quality, they sometimes simulate disease or mask pathologic abnormalities. Several techniques are available that help to minimize or avoid artifacts. For the personnel running the MR scanner it is crucial to know about potential sources and the physical basis of artifacts. Investigations of origins and effects of artifacts not only can lead to further understand the process of MR imaging, but can also help to find new MRI methods.

Conflict of Interest Statement

We certify that there is no actual or potential conflict of interest in relation to this article.

References

1. Arena L, Morehouse HT, Safir J. MR imaging artifacts that simulate disease: how to recognize and to eliminate them. *Radiographics* 1995; 15:1373–94.
2. Smith AS, Weinstein MA, Hurst GC, et al. Intracranial chemical-shift artifacts on MR images of the brain: observations and relation to sampling bandwidth. *AJR Am J Roentgenol* 1990;154:1275–83.
3. Savci G, Yazici Z, Sahin N, et al. Value of chemical shift subtraction MRI in characterization of adrenal masses. *AJR Am J Roentgenol* 2006; 186:130–5.
4. Czervionke LF, Czervionke JM, Daniels DL, et al. Characteristic features of MR truncation artifacts. *AJR Am J Roentgenol* 1988;151:1219–28.
5. Ehman RL, Felmlee JP. Flow artifact reduction in MRI: a review of the roles of gradient moment nulling and spatial presaturation. *Magn Reson Med* 1990;14:293–307.
6. Ordidge RJ, Helpert JA, Qing ZX, et al. Correction of motional artifacts in diffusion-weighted MR images using navigator echoes. *Magn Reson Imaging* 1994;12:455–60.
7. Pipe JG. Motion correction with PROPELLER MRI: application to head motion and free-breathing cardiac imaging. *Magn Reson Med* 1999; 42:963–9.
8. Zand KR, Reinhold C, Haider MA, et al. Artifacts and pitfalls in MR imaging of the pelvis. *J Magn Reson Imaging* 2007;26:480–97.
9. Deichmann R, Josephs O, Hutton C, et al. Compensation of susceptibility-induced BOLD sensitivity losses in echo-planar fMRI imaging. *Neuroimage* 2002;15:120–35.
10. Delfaut EM, Beltran J, Johnson G, et al. Fat suppression in MR imaging: techniques and pitfalls. *Radiographics* 1999;19:373–82.
11. Zur Y, Wood ML, Neuringer LJ. Spoiling of transverse magnetization in steady-state sequences. *Magn Reson Med* 1991;21:251–63.
12. Davis WL, Warnock SH, Harnsberger HR, et al. Intracranial MRA: single volume vs. multiple thin slab 3D time-of-flight acquisition. *J Comput Assist Tomogr* 1993;17:15–21.

13. Atkinson D, Brant-Zawadzki M, Gillan G, et al. Improved MR angiography: magnetization transfer suppression with variable flip angle excitation and increased resolution. *Radiology* 1994;190:890-4.
14. Anzalone N, Scomazzoni F, Castellano R, et al. Carotid artery stenosis: intraindividual correlations of 3D time-of-flight MR angiography, contrast-enhanced MR angiography, conventional DSA, and rotational angiography for detection and grading. *Radiology* 2005;236:204-13.
15. Papadakis NG, Martin KM, Pickard JD, et al. Gradient preemphasis calibration in diffusion-weighted echo-planar imaging. *Magn Reson Med* 2000;44:616-24.
16. Schmithorst VJ, Dardzinski BJ, Holland SK. Simultaneous correction of ghost and geometric distortion artifacts in EPI using a multiecho reference scan. *IEEE Trans Med Imaging* 2001;20:535-9.
17. Jezzard P, Barnett AS, Pierpaoli C. Characterization of and correction for eddy current artifacts in echo planar diffusion imaging. *Magn Reson Med* 1998;39:801-12.
18. Chen NK, Wyrwicz AM. Optimized distortion correction technique for echo planar imaging. *Magn Reson Med* 2001;45:525-8.
19. Collins CM, Liu W, Schreiber W, et al. Central brightening due to constructive interference with, without, and despite dielectric resonance. *J Magn Reson Imaging* 2005;21:192-6.
20. Setsompop K, Wald LL, Alagappan V, et al. Parallel RF transmission with eight channels at 3 Tesla. *Magn Reson Med* 2006;56:1163-71.
21. Thomas DL, De Vita E, Deichmann R, et al. 3D MDEFT imaging of the human brain at 4.7 T with reduced sensitivity to radiofrequency inhomogeneity. *Magn Reson Med* 2005;53:1452-8.
22. Saekho S, Yip CY, Noll DC, et al. Fast-kz three-dimensional tailored radiofrequency pulse for reduced B1 inhomogeneity. *Magn Reson Med* 2006;55:719-24.
23. Patel MR, Siewert B, Warach S, et al. Diffusion and perfusion imaging techniques. *Magn Reson Imaging Clin N Am* 1995;3:425-38.
24. Haacke EM, Xu Y, Cheng YC, et al. Susceptibility weighted imaging (SWI). *Magn Reson Med* 2004;52:612-8.
25. Le Bihan D. The "wet mind": water and functional neuroimaging. *Phys Med Biol* 2007;52:57-90.

Address for Correspondence

Professor Sabine Heiland, PhD
Division of Experimental Radiology
Department of Neurology
University of Heidelberg Medical Center
Im Neuenheimer Feld 400
69120 Heidelberg
Germany
Phone (+49/6221) 56-7566, Fax -4673
e-mail: sabine.heiland@med.uni-heidelberg.de